

NEXT-TO-LEADING ORDER CONSTITUENT QUARK STRUCTURE AND HADRONIC STRUCTURE FUNCTIONS

Firooz Arash^{(a,b,c)*}and Ali N. Khorramian^{(c,d)†}

^(a) Center for Theoretical Physics and Mathematics, AEOI,
P.O. Box 11365-8486, Tehran, Iran

^(b) Physics Department, AmirKabir University (Tafresh Campus),
Hafez Ave., Tehran Iran 19834

^(c) Institute for Studies in Theoretical Physics and Mathematics
P.O.Box 19395-5531, Tehran, Iran

^(d) Physics Department, Semnan University, Semnan, Iran,

November 3, 2018

Abstract

We calculate the partonic structure of a constituent quark in the Next-to-Leading Order framework. The structure of any hadron can be obtained thereafter using a convolution method. Such a procedure is used to generate the structure function of proton and pion in NLO, neglecting certain corrections to Λ_{QCD} . It is shown that while the constituent quark structure is generated purely perturbatively and accounts for the most part of the hadronic structure, there is a few percent contributions coming

*farash@cic.aut.ac.ir

†khorramiana@theory.ipm.ac.ir

from the nonperturbative sector in the hadronic structure. This contribution plays the key role in explaining the $SU(2)$ symmetry breaking of the nucleon sea and the observed violation of Gottfried sum rule. These effects are calculated. We obtained an Excellent agreement with the experimental data in a wide range of $x = [10^{-6}, 1]$ and $Q^2 = [0.5, 5000] \text{ GeV}^2$ for the proton structure function. We have also calculated Pion structure and compared it with the existing data. Again, the model calculations agree rather well with the data from experiment. **PACS Numbers:** **13.60 Hb, 12.39.-x, 13.88 +e, 12.20.Fv**

1 INTRODUCTION

Our knowledge of hadronic structure is based on the hadron spectroscopy and the Deep Inelastic Scattering (DIS) data. In the former picture quarks are massive particles and their bound states describe the static properties of hadrons. On the other hand, the interpretation of DIS data relies upon the quarks of QCD Lagrangian with very small mass. The hadronic structure in this picture is intimately connected with the presence of a large number of partons (quarks and gluons). Mass is not the only difference between these two types of quarks; they also differ in other important properties. For example, the color charge of quark field in QCD Lagrangian is ill-defined and is not gauge invariant, reflecting the color of gluons in an interacting theory; whereas, color associated with a constituent quark (CQ) is a well defined entity. It is shown that [1][2] one can perturbatively dress a QCD Lagrangian field to all orders and construct a CQ in conformity with the color confinement. From this point of view a CQ is defined as a quasi-particle emerging from the dressing of valence quark with gluons and $q - \bar{q}$ pairs in QCD.

Of course, the concept of CQ as an intermediate step between the quarks of QCD Lagrangian and hadrons is not new. In fact, Altarelli and Cabibo [3] used this concept in the context of $SU(6) \times O(3)$. R.C. Hwa in his work used the term *valon*, for them, elaborated on the concept and showed its applications to many physical processes [4]. In Ref.[2] it

is suggested that the concept of dressed quark and gluon might be useful in the area of jet physics and heavy quark effective theory. Despite the ever presence of CQ no one has calculated its content and partonic structure without resorting to hadronic data and the process of deconvolution. Thus, the purpose of this paper is threefold: (a) to evaluate the structure of a CQ in the Next-to-Leading Order (NLO) framework of QCD, (b) to verify its conformity with the structure function data of nucleon and pion for which ample data are available, (c) to include additional refinements that are needed to account for the violation of Gottfried Sum Rule (GSR) and the binding effect of constituent quarks to form a physical hadron.

2 FORMALISM

2.1 Moments of Parton Distribution in a CQ

In this subsection we will utilize the extended work done on the development of the NLO calculations of moments, to calculate the structure of a constituent quark. What will follow in the rest of this subsection is not a new next-to-leading order calculation. However, we find it interesting to explore the existing calculations in the valon framework.

By definition, a CQ is a universal building block for every hadron; that is, the structure of a CQ is common to all hadrons and is generated perturbatively. Once its structure is calculated, it would be possible, in principle, to calculate the structure of any hadron. In doing so, we will follow the philosophy that in a DIS experiment at high enough Q^2 , it is the structure of a CQ which is being probed, and that at sufficiently low value of Q^2 this structure cannot be resolved. Thus, a CQ behaves as a valence quark, and a hadron is viewed as the bound state of its constituent quarks. Under these criteria, partons of DIS experiments are components of CQ. The structure function of a U-type CQ at high Q^2

can be written as[4]:

$$F_2^U(z, Q^2) = \frac{4}{9}z(G_{\frac{u}{U}} + G_{\frac{\bar{u}}{U}}) + \frac{1}{9}z(G_{\frac{d}{U}} + G_{\frac{\bar{d}}{U}} + G_{\frac{s}{U}} + G_{\frac{\bar{s}}{U}}) + \dots \quad (1)$$

where all the functions on the right-hand side are the probability functions for quarks having momentum fraction z of a U-type CQ at Q^2 . A similar expression can be written for a D-type CQ. Following Ref. [4], we define the singlet (S) and nonsinglet (NS) components of the CQ structure functions as:

$$G^S = \sum_{i=1}^f (G_{\frac{q_i}{CQ}} + G_{\frac{\bar{q}_i}{CQ}}) = G_f + (2f - 1)G_{uf} \quad (2)$$

$$G^{NS} = \sum_{i=1}^f (G_{\frac{q_i}{CQ}} - G_{\frac{\bar{q}_i}{CQ}}) = G_f - G_{uf} \quad (3)$$

where G_f is the favored distribution describing the structure function of a quark within a CQ of the same flavor, while the unfavored distribution, G_{uf} , describes the structure function of any quark of different flavor within the CQ. We have used, f , for the number of active flavors. Solving (2) and (3) for G_f and G_{uf} , we get,

$$G_f = \frac{1}{2f}(G^S + (2f - 1)G^{NS}), \quad (4)$$

$$G_{uf} = \frac{1}{2f}(G^S - G^{NS}). \quad (5)$$

Having expressed all the structure functions of a CQ in terms of G_f and G_{uf} , we now go to the N- moment space and define the moments of these distributions as:

$$M_2(N, Q^2) = \int_0^1 x^{N-2} F_2(x, Q^2) dx \quad (6)$$

$$M_i(N, Q^2) = \int_0^1 x^{N-1} G_i(x, Q^2) dx \quad (7)$$

where, the subscription i stands for S or NS. Due to charge symmetry, in the following, we only write the CQ distribution for proton.

In the NLO approximation the dependence of the running coupling constant, α_s , on Q^2 is given by:

$$\alpha_s(Q^2) \approx \frac{4\pi}{\beta_0 \ln(\frac{Q^2}{\Lambda^2})} \left(1 - \frac{\beta_1 \ln \ln(\frac{Q^2}{\Lambda^2})}{\beta_0^2 \ln(\frac{Q^2}{\Lambda^2})}\right), \quad (8)$$

with $\beta_0 = \frac{1}{3}(33 - 2f)$ and $\beta_1 = 102 - \frac{38f}{3}$. The evolution of parton distributions is controlled by the anomalous dimensions:

$$\gamma_{NS}^N = \frac{\alpha_s}{4\pi} \gamma_{qq}^{(0)N} + \left(\frac{\alpha_s}{4\pi}\right)^2 \gamma_{NS}^{(1)N} \quad \gamma_{ij}^N = \frac{\alpha_s}{4\pi} \gamma_{ij}^{(0)N} + \left(\frac{\alpha_s}{4\pi}\right)^2 \gamma_{ij}^{(1)N}$$

where $i, j = q, g$; and $\gamma^{(0,1)N}$ are one and two loop anomalous dimension matrices. The nonsinglet moments in the NLO are as follows:

$$M^{NS}(N, Q^2) = [1 + \frac{\alpha_s(Q^2) - \alpha_s(Q_0^2)}{4\pi} \left(\frac{\gamma_{NS}^{(1)N}}{2\beta_0} - \frac{\beta_1 \gamma_{qq}^{(0)N}}{2\beta_0^2} \right)] \left(\frac{\alpha_s(Q^2)}{\alpha_s(Q_0^2)} \right)^{\frac{\gamma_{qq}^{(0)N}}{2\beta_0}}. \quad (9)$$

The anomalous dimension matrices, $\gamma^{(0,1)N}$, are given by,

$$\gamma^{(0,1)N} = \begin{pmatrix} \gamma_{qq}^{(0,1)N} & \gamma_{qg}^{(0,1)N} \\ \gamma_{gq}^{(0,1)N} & \gamma_{gg}^{(0,1)N} \end{pmatrix} \quad (10)$$

These matrices, govern the moments of the singlet quark and sector as given by:

$$\begin{pmatrix} M^S(N, Q^2) \\ M^G(N, Q^2) \end{pmatrix} = \left\{ \left(\frac{\alpha_s(Q^2)}{\alpha_s(Q_0^2)} \right)^{\frac{\lambda_-^N}{2\beta_0}} [p_-^N - \frac{1}{2\beta_0} \frac{\alpha_s(Q_0^2) - \alpha_s(Q^2)}{4\pi} p_-^N \gamma^N p_-^N - \right. \right. \\ \left. \left. \left(\frac{\alpha_s(Q_0^2)}{4\pi} - \frac{\alpha_s(Q^2)}{4\pi} \left(\frac{\alpha_s(Q^2)}{\alpha_s(Q_0^2)} \right)^{\frac{\lambda_+^N - \lambda_-^N}{2\beta_0}} \right) \frac{p_-^N \gamma^N p_+^N}{2\beta_0 + \lambda_+^N - \lambda_-^N} \right] \right\} \mathbf{1} + \{(\mathcal{Q}_{+\longleftrightarrow-})\} \quad (11)$$

where $\gamma^N = \gamma^{(1)N} - \frac{\beta_1}{\beta_0} \gamma^{(0)N}$ and $\gamma^{(0)N}$, $\gamma^{(1)N}$ are one and two-loop anomalous dimension matrices, respectively. $\mathbf{1}$ is the unit matrix. Notice that the last term in Eq. (11), $\mathcal{Q}_{+\longleftrightarrow-}$, means that all subscripts are exchanged. The leading order behavior is obtained from the first term in the square brackets. λ_{\pm}^N denote the eigenvalues of the one-loop anomalous dimension matrix, $\gamma^{(0)N}$:

$$\lambda_{\pm}^N = \frac{1}{2} [\gamma_{qq}^{(0)N} + \gamma_{gg}^{(0)N} \pm \sqrt{(\gamma_{gg}^{(0)N} - \gamma_{qq}^{(0)N})^2 + 4\gamma_{qg}^{(0)N} \gamma_{gq}^{(0)N}}] \quad (12)$$

These anomalous dimensions and $\gamma_{kl}^{(1,0)N}$ are calculated up to second order in α_s and can be found in [5] [6]. p_{\pm}^N are as follows:

$$p_{\pm}^N = \pm(\gamma^{(0)N} - \lambda_{\mp}^N) / (\lambda_+^N - \lambda_-^N) \quad (13)$$

In Ref. [4], $d_{\pm}^{(0)}$ is used to denote the leading order anomalous dimensions; these are related to λ_{\pm} by: $d_{\pm}^0 = \frac{\lambda_{\pm}^N}{2\beta_0}$.

In evaluating these moments, we have taken $Q_0^2 = 0.283 \text{ GeV}^2$ and $\Lambda = 0.22 \text{ GeV}$, as our initial scales. It seems that evolution of parton distributions from such a low value of Q_0^2 is not justified theoretically; we shall take up this issue shortly in subsection 2.3.

2.2 Parton Densities In CQ

In the previous subsection we outlined how to calculate the moments. In this subsection we will give the corresponding parton distributions in a CQ.

The moments of the CQ structure function, $F_2^{CQ}(z, Q^2)$, are expressed completely in terms of Q^2 through the evolution parameter t :

$$t = \ln \frac{\ln \frac{Q^2}{\Lambda^2}}{\ln \frac{Q_0^2}{\Lambda^2}} \quad (14)$$

The moments of valence and sea quarks in a CQ are,

$$M_{\frac{\text{valence}}{CQ}} = M^{NS}(N, Q^2) \quad (15)$$

$$M_{\frac{\text{sea}}{CQ}} = \frac{1}{2f}(M^S - M^{NS}) \quad (16)$$

where $M^{S,NS}$ are given by eqs. (9) and (11). It is now straightforward, to evaluate $M_{\frac{\text{valence}}{CQ}}$ and $M_{\frac{\text{sea}}{CQ}}$ at any Q^2 or t . These are calculated numerically for a range of N at fixed Q^2 or t . In Figure (1) we present these moments both in the leading and next-to-leading orders. For every value of t we fit the moments by a beta function, which in turn is the moment of the parton distribution as given below,

$$zq_{\frac{\text{val.}}{CQ}}(z, Q^2) = az^b(1-z)^c \quad (17)$$

$$zq_{\frac{\text{sea}}{CQ}}(z, Q^2) = \alpha z^\beta(1-z)^\gamma[1 + \eta z + \xi z^{0.5}] \quad (18)$$

The parameters $a, b, c, \alpha, \beta, \gamma, \eta$, and ξ are functions of Q^2 through the evolution parameter t . The same form as in Eq. (18) is obtained for the gluon distribution in a CQ, only with different parameter values. The functional forms of these parameters are polynomials of order three in t and are given in the appendix. The goodness of these we fits are checked

by χ^2 minimization procedure. We find that, for all parameters a , b , c , and d , of the valence quark sector $\chi^2/DOF = 0.99$, with the standard error of order 10^{-3} . For the sea quark and gluon sector, χ^2/DOF carries between 0.91 and 0.98. Of course, the forms (17) and (18) are not unique; rather, they are the most simple and commonly used forms. We note that the sum rule reflecting the fact that each CQ contains only one valence quark is satisfied at all values of Q^2 :

$$\int_0^1 q_{\frac{\text{val.}}{\text{CQ}}}(z, Q^2) dz = 1. \quad (19)$$

Substituting these results into Eq. (1) completes the evaluation of CQ structure function in NLO. In Figure (2), we plot various parton distributions inside a CQ.

2.3 discussion

In subsection 2.1 we indicated that our initial scales are $Q_0^2 = 0.283 \text{ GeV}^2$ and $\Lambda = 0.22 \text{ GeV}$. The above value of Q_0 corresponds to a distance of 0.36 fm which is roughly equal to or slightly less than the radius of a CQ. It may be objected that such distances are probably too large for a meaningful pure perturbative treatment. We note that $F_2^{\text{CQ}}(z, Q^2)$ has the property that it becomes $\delta(z - 1)$ as Q^2 is extrapolated to Q_0^2 , which is beyond the region of validity. This mathematical boundary condition signifies that the internal structure of a CQ cannot be resolved at Q_0 in the NLO approximation. Consequently, when this property is applied to Eq.(20), below, the structure function of the nucleon becomes directly related to $xG_{\frac{\text{CQ}}{P}}(x)$ at those values of Q_0 ; that is, Q_0 is the leading order effective value at which the hadron can be considered as consisting of only three (two) CQ, for baryons (mesons). We have checked that when Q^2 approaches to Q_0^2 the quark moments approach to unity and the moments of gluon approach to zero. In fact for $Q^2 = 0.2839$ gluon moments are at the order of 10^{-4} and singlet and nonsinglet moments are 0.9992. In fact our results are only meaningful for $Q_0^2 \geq 0.4 \text{ GeV}^2$.

From the theoretical standpoint, both Λ and Q_0 depend on the order of the moments, N ;

but here, we have assumed that they are independent of N . In this way, we have introduced some degree of approximation to the Q^2 evolution of the valence and sea quarks. However, on one hand there are other contributions like target-mass effects, which add uncertainties to the theoretical predictions of perturbative QCD, while on the other hand since we are dealing with the CQ, there is no experimental data to invalidate an N independent Λ assumption.

3 HADRONIC STRUCTURE

3.1 Constituent Quark Distribution in hadron

So far, the structure of a CQ is calculated in the NLO framework. In this section we will use the convolution method to calculate the structure functions of proton, $F_2^p(x, Q^2)$, and pion. Let us denote the structure function of a CQ by $F_2^{CQ}(z, Q^2)$ and the probability of finding a CQ carrying momentum fraction y of the hadron by $G_{\frac{CQ}{h}}(y)$. The corresponding structure function of a hadron is obtained by convolution of $F_2^{CQ}(z, Q^2)$ and $G_{\frac{CQ}{h}}(y)$,

$$F_2^h(x, Q^2) = \sum_{CQ} \int_x^1 dy G_{\frac{CQ}{h}}(y) F_2^{CQ}\left(\frac{x}{y}, Q^2\right) \quad (20)$$

where summation runs over the number of CQ's in a particular hadron. We note that $G_{\frac{CQ}{h}}(y)$ is independent of the nature of the probe, and its Q^2 value. In effect $G_{\frac{CQ}{h}}(y)$ describes the wave function of hadron in CQ representation, containing all the complications due to confinement. From the theoretical point of view, this function cannot be evaluated accurately. To facilitate phenomenological analysis, following [4], we assume a simple form for the exclusive CQ distribution in proton and pion as follows,

$$G_{UU D/p}(y_1, y_2, y_3) = l(y_1 y_2)^m y_3^n \delta(y_1 + y_2 + y_3 - 1) \quad (21)$$

$$G_{\bar{U} D/\pi^-}(y_1, y_2) = q y_1^\mu y_2^\nu \delta(y_1 + y_2 - 1) \quad (22)$$

where l and q are normalization parameters. After integrating over unwanted momenta, we can arrive at the inclusive distribution of individual CQ:

$$G_{U/p}(y) = \frac{1}{B(m+1, n+m+2)} y^m (1-y)^{m+n+1}, \quad (23)$$

$$G_{D/p}(y) = \frac{1}{B(n+1, 2m+2)} y^n (1-y)^{2m+1}, \quad (24)$$

$$G_{\bar{U}/\pi^-}(y) = \frac{1}{B(\mu+1, \nu+1)} y^\mu (1-y)^\nu. \quad (25)$$

Similar expression for G_{D/π^-} is obtained with the interchange of $\mu \leftrightarrow \nu$. In the above equations, $B(i, j)$ is the Euler Beta function. The arguments of this function, as well as, l and q of Eqs.(21) and (22), are fixed by the number and momentum sum rules:

$$\int_0^1 G_{\frac{CQ}{h}}(y) dy = 1, \quad \sum_{CQ} \int_0^1 y G_{\frac{CQ}{h}}(y) dy = 1, \quad (26)$$

where $CQ = U, D, \bar{U}$ and $h = p, \pi^-$. Numerical values are: $\mu = 0.01$, $\nu = 0.06$, $m = 0.65$ and $n = 0.35$. These parameters are independent of Q^2 and are given in [4] and [7] for proton and pion, respectively. In [8], a new set of values for m and n are suggested which differ significantly from the values quoted above. Reference [8] uses the CTEQ parton distributions in the Next-to-Leading order to fix these parameters. The authors of Ref. [8] have found yet another set of values in [9], which differs from those given in [4] and [8]. They attribute these differences to the different theoretical assumptions. We have tried a range of values for m , n , ν and μ , and checked that the sum rules (26) are satisfied. Because of the Beta function in the denominator of Eqs.(23-25) the number sum rule does not change by changing m and n and we found little sensitivity on the momentum sum rule. In Fact, we have varied both m and n , randomly in the interval $[0.2, 1.95]$, and checked it against F_2^p data. We found very little sensitivity to the choices made. For the data that we shall analyze, these two parameter formulas will prove to be adequate. The differences between parameters of Ref. [8] and Ref. [4] (which we have adopted) can be attributed to the different methods of extracting the parameters. We have calculated

the parton distributions from the perturbative QCD, whereas Ref.[8] have used CTEQ's global fit to extract parton content of nucleon.

The considerations on the form of CQ distribution that are used here, does not exclude other possibilities. However, in our model the quark distribution, say, in a proton is described as the convolution of the CQ distribution, $G_{\frac{CQ}{p}}$, and the quark distribution in the CQ. In the moment form the latter two become the product of their moments. Mathematically, these two moments can be modified without changing the product. That would, of course, modify the original $G_{\frac{CQ}{p}}$ and parton distribution in a CQ. But the parton distribution has a definite meaning. It is the evolution of a quark as Q increases. At $Q = Q_0$, parton distribution is a delta function, implying that the CQ has no internal structure that can be probed. Our model is to say that the three valence quark at high Q becomes three CQ's at low Q without anything else. Such a physical statement of the model does not permit to redefine $G_{\frac{CQ}{p}}$ or the parton distribution in a CQ, although mathematical criticism still remains.

Our choice of $G_{\frac{CQ}{p}}$ is sufficient to fit all the data of deep inelastic scattering in the range of interest. It does not mean that a more complicated $G_{\frac{CQ}{p}}$ is ruled out. It is a subject that can be revisited in the future when problem arise. At this point our formula for the CQ distribution is satisfactory. A comment regarding the moments is in order: The definition of the moments are not arbitrary if we are to attach physical interpretation to the constituent quark distribution. There are only two U and one D in a proton, which impose constrains on the first moment. Also, the sum of the CQ momenta should be one, which imposes a constraint on the second moment. If one writes the valence quark moments as a product of G_n and M^{NS} then M^{NS} must have connection with QCD evolution to ensure that there is only one valence quark in every CQ and hence, the constraint becomes $M_1^{NS} = 1$. With these constrains, one cannot freely redefine moments of CQ distribution, M^{NS} and M^S . yet, there are infinite number of CQ moments and we have cited only two constraints. Does this leave an infinite horde number of undefined quantities? The higher

moments of the CQ distribution are affected mainly by the large x behavior of proton wave function, or will affect only the even larger x behavior of the parton distribution. Until one focuses on that region and finds inconsistency, one chooses the simplest parameterization. There are similar situations both in classical and contemporary physics. The question can be turned around and asked why did Newton stop at $\frac{1}{r^2}$ law for gravitational force? Could he have excluded the possible existence of $\frac{1}{r^n}$ terms with $n = 3, 4, 5, \dots$? By only citing the existence of two constraints, Newton avoided confronting the infinite horde of undefined quantities. Our model is inductive physics. Valons or CQ's are not derived by deductive logic from the first principles. In modeling, one finds the simplest way to capture the essence of the physics involved. The situation is also present in contemporary physics: we could have asked why the Cornell potential for the bound-state problem of quark and antiquark does not contain all possible power law terms beside the $\frac{1}{r}$ and the r terms. The answer is simple: it is what fits the particle mass spectrum that counts, again in the simplest way possible that captures the essence of the problem.

3.2 Parton distribution in hadrons

Having specified the parton distributions in the CQ and the constituent quark distribution in proton and pion, it is possible to determine various parton distributions in any hadron. For proton, we get:

$$q_{val./p}(x, Q^2) = 2 \int_x^1 \frac{dy}{y} G_{U/p}(y) q_{val./U}\left(\frac{x}{y}, Q^2\right) + \int_x^1 \frac{dy}{y} G_{D/p}(y) q_{val./D}\left(\frac{x}{y}, Q^2\right) = u_{val./p}(x, Q^2) + d_{val./p}(x, Q^2) \quad (27)$$

$$q_{sea/p}(x, Q^2) = 2 \int_x^1 \frac{dy}{y} G_{U/p}(y) q_{sea/U}\left(\frac{x}{y}, Q^2\right) + \int_x^1 \frac{dy}{y} G_{D/p}(y) q_{sea/D}\left(\frac{x}{y}, Q^2\right) \quad (28)$$

The above equations represent the contribution of constituent quarks to the sea and the valence quark distributions in proton. In Figure (3), the CQ contribution to parton

distributions in p and π^- is shown. Comparing with proton structure function data, shows that the results fall short of representing the experimental data by a few percent (3%-8%, depending on Q^2 and x). This is not surprising, for it is a well established fact that there are soft gluons in the nucleon. We attribute their presence to the fact that constituent quarks are not free in a hadron, but interact with each other to form the bound states. At each Q^2 value we have computed the soft gluon contribution using direct comparison with experimental data. The final result is parameterized as:

$$xg_{soft} = R(Q^2)x^{-0.029}(1-x)^{2.79}; \quad (29)$$

where, $R(Q^2) = 2.14 - 6.13t + 6.177t^2 - 1.812t^3$. In figure (4), the shape of xg_{soft} is presented for a range of Q^2 values. Splitting of these gluons could in turn produce $\bar{q} - q$ pairs which can combine with the original constituent quarks and fluctuate the baryonic state to a meson-baryon state. This also will break the $SU(2)$ symmetry of the sea as we shall see next.

3.3 The Role of Soft Gluon

In our model there is no room in the CQ structure for the breaking of $SU(2)$ symmetry of the nucleon sea. But, after creation of $\bar{q} - q$ pair by the soft gluons, these quarks can recombine with CQ to fluctuate into meson-nucleon state which breaks the symmetry of the nucleon sea. In what follows we will compute this component, and its contribution to the nucleon structure function, and its relevance to the violation of the Gottfried sum rule. We will follow the prescription of [10] and [11]. The above proposed model, is similar to the effective chiral quark theory, in which the relevant degrees of freedom are constituent quarks, gluons and Goldstone bosons. The coupling of pions produces pion cloud of the constituent quark, in which we are interested. The point we would like to make is that, there are two types of sea quark and gluon that contribute to the nucleon sea measured

in DIS. One type is generated from QCD hard bremsstrahlung and gluon splitting. This component is discussed in subsection 2.2 and is associated with the internal composition of the constituent quark rather than the proton itself. The other contribution is generated nonperturbatively via meson-baryon fluctuation. As we will show, according to our results, this component provides a consistent framework to understand the flavor asymmetry of the nucleon sea. It also compensates for the shortcoming of perturbatively generated parton densities in reproducing the experimental data on F_2^p . In order to distinguish these partons from those confined inside the CQ, we will term them as *inherent* partons. This component is intimately related to the bound state problem, and hence it has a non-perturbative origin. However, for the process of $CQ \rightarrow CQ + \text{gluon} \rightarrow \bar{q} - q$, at an initial value of $Q^2 = 0.65 \text{GeV}^2$ where α_s is still small enough, we will calculate it perturbatively. The corresponding splitting functions are as follows,

$$P_{gq}(z) = \frac{4}{3} \frac{1 + (1 - z)^2}{z}, \quad (30)$$

$$P_{qg}(z) = \frac{1}{2}(z^2 + (1 + z)^2). \quad (31)$$

For the joint probability distribution of the process at hand, we get,

$$q_{inh.}(x, Q^2) = \bar{q}_{inh}(x, Q^2) = \mathcal{N} \frac{\alpha_s}{(2\pi)} \int_x^1 \frac{dy}{y} P_{qg}\left(\frac{x}{y}\right) g_{soft}(y) dy \quad (32)$$

where $q_{inh.}$ is the inherent parton density. The splitting functions, and the $q_{inh}(x, Q^2) = (\bar{q}_{inh}(x, Q^2))$, are those of the leading order, rather than NLO. We do not expect that this approximation will affect the whole structure function, as can be seen from Figure (5). In the above equation \mathcal{N} , is a factor depending on Q^2 , and G_{CQ} is the constituent quark distribution in the proton as given previously. The same process, can also be a source of $SU(2)$ symmetry breaking of nucleon sea; namely, $u_{sea} \neq d_{sea}$, and hence, the violation of the Gottfried sum rule (GSR). We will take up this issue in the next subsection.

The process is depicted in Figure (6). Probability to form a meson-baryon state can be

written as in Ref. [11],

$$P_{MB}(x) = \int_0^1 \frac{dy}{y} \int_0^1 \frac{dz}{z} F(y, z) R(y, z; x) \quad (33)$$

where $F(y, z)$ is the joint probability of finding a CQ with momentum fraction y , and an inherent quark or anti-quark of momentum fraction z in the proton. $R(y, z; x)$ is the probability of recombining a CQ of momentum y , with an inherent quark of momentum z , to form a meson of momentum fraction x in the proton. For a more general case, the evaluation of both of these probability functions are discussed in [12]. An earlier and pioneering version was proposed in [13]. In the present case, these functions are much simpler. Guided by the works of Ref. [11, 12, 13], we can write,

$$F(y, z) = \Omega y G_{\frac{CQ}{p}}(y) z \bar{q}_{inh.}(z) (1 - y - z)^\delta \quad (34)$$

$$R(y, z; x) = \rho y^a z^b \delta(y + z - 1) \quad (35)$$

Here, we take $a = b = 1$ reflecting that the two CQ's in meson share its momentum almost equally. The exponent δ is fixed for the n and Δ^{++} states, using the data from E866 experiment [14], and the mass ratio of Δ to n . They turn out to be approximately 18 and 13, respectively. Ω and ρ are the normalization constants, also fixed by data. We recognize that the discussion leading to Eqs. (34, 35) and fixing the parameters are based on a phenomenological ansatz. The ansatz and the parameters of Eqs. (34, 35) seems working remarkably well, and further effects that might be of hadronic origin need not be larger than a few percent.

Now it is possible to evaluate \bar{u}_M and \bar{d}_M quarks, associated with the formation of meson states[11]:

$$\bar{d}_M(x, Q^2) = \int_x^1 \frac{dy}{y} [P_{\pi^+ n}(y) + \frac{1}{6} P_{\pi^+ \Delta^0}(y)] \bar{d}_\pi(\frac{x}{y}, Q^2) \quad (36)$$

$$\bar{u}_M(x, Q^2) = \frac{1}{2} \int_x^1 \frac{dy}{y} P_{\pi^- \Delta^{++}}(y) \bar{u}_\pi(\frac{x}{y}, Q^2) \quad (37)$$

where \bar{u}_π and \bar{d}_π are the valence quark densities in the pion at scale Q_0^2 . The coefficients $\frac{1}{2}$ and $\frac{1}{6}$ are due to isospin consideration. Using Eqs. (17), (18), and (25), we can calculate

various parton distributions in a pion. Those pertinent to Eqs. (35) and (36) are:

$$\bar{u}_{val.}^{\pi^-}(x, Q^2) = \int_x^1 G_{\bar{U}/\pi^-}(y) \bar{u}_{val./\bar{U}}\left(\frac{x}{y}, Q^2\right) \frac{dy}{y}, \quad (38)$$

$$d_{val.}^{\pi^-}(x, Q^2) = \int_x^1 G_{D/\pi^-}(y) d_{val./D}\left(\frac{x}{y}, Q^2\right) \frac{dy}{y}, \quad (39)$$

$$\bar{u}_{val./\bar{U}} = u_{val./U}. \quad (40)$$

There are some data on the valence structure function of π^- [15], which can serve as a check for the proposed model. Defining valence structure function of π^- as

$$F_{val.}^{\pi^-} = x \bar{u}_{val.}^{\pi^-} = x d_{val.}^{\pi^-}. \quad (41)$$

We present the results of our calculation for $F_{val.}^{\pi^-}$ in Figure (7), along with the experimental data at Q^2 around 6 Gev^2 .

3.4 Asymmetry of the Nucleon Sea and the Gottfried Sum Rule

There are experimental evidences [14],[16] that the Gottfried integral,

$$S_G = \int_0^1 [F_2^p(x) - F_2^n(x)] \frac{dx}{x} = \frac{1}{3} - \frac{2}{3} \int_0^1 dx [\bar{d}(x) - \bar{u}(x)], \quad (42)$$

is less than $\frac{1}{3}$ which is the value expected in the simple quark model. The NMC collaboration [16], result at $Q^2 = 4 GeV^2$ is, $S_G = 0.235 \pm 0.026$, which is significantly smaller than $\frac{1}{3}$. There are several explanations for this observed violation of the Gottfreid sum rule (GSR). Among them are: flavor asymmetry of the nucleon sea, that is, $\bar{u}_{sea} \neq \bar{d}_{sea}$,[17] [18], isospin symmetry breaking between proton and neutron, and Pauli blocking, among others. One of these explanations fits well within our model.

It was proposed by Eichten, Inchliffe, and Quigg [19], that valence quark fluctuates into a quark and a pion. This explanation fits very well in our model. In other words, a nucleon can fluctuate into a meson-nucleon state. The idea is appealing to us and in our model it can be calculated rather easily. According to our model, after a pair of *inherent* $q - \bar{q}$, is created, a \bar{u} can couple to a D-type CQ to form an intermediate $\pi^- = D\bar{u}$, while the

u quark combines with the other two U-type CQ's to form a Δ^{++} . This is the lowest $u\bar{u}$ fluctuation. Similarly, a $d\bar{d}$ can fluctuate into the π^+n state. Since the Δ^{++} state is more massive than the n state, the probability of $d\bar{d}$ fluctuation will dominate over $u\bar{u}$ fluctuation, which naturally leads to an excess of $d\bar{d}$ pairs over $u\bar{u}$ in the proton sea. This process is depicted in Figure (6).

To summarize, there are three sources that contribute to the sea partons in the proton: Constituent quarks of the proton, the mesonic cloud of the CQ, and the splitting of soft gluon. The combined contribution to the ratio of $\frac{\bar{d}}{\bar{u}}$ is as follows:

$$(\frac{\bar{d}}{\bar{u}})_{proton} = \frac{\bar{d}_M + \bar{d}_{inh.+CQ}}{\bar{u}_M + \bar{u}_{inh.+CQ}}. \quad (43)$$

NUSea collaboration at FermiLab, E866 experiment, has published their results [14], for the integral of $\bar{d} - \bar{u}$ and $\frac{\bar{d}}{\bar{u}}$ at $Q = 7.35 \text{ GeV}$. With the procedure described, we have calculated these values at the same Q and for the same range of x , that is, $x = [0.02, 0.35]$.

The result of the model is,

$$\int_{0.02}^{0.345} dx(\bar{d} - \bar{u}) = 0.085, \quad (44)$$

to be compared with the experimental value of 0.068 ± 0.0106 . For the entire range in x , we get: $\int_0^1 dx(\bar{d} - \bar{u}) = 0.103$. The corresponding experimentally extrapolated value is 0.1 ± 0.018 , which is in excellent agreement with our calculations. At $Q = 7.35 \text{ GeV}$, this gives $S_G = 0.264$. In Figure (8), $\bar{d}(x) - \bar{u}(x)$ and $\frac{\bar{d}}{\bar{u}}$ in the proton are shown as a function of x at $Q = 7.35 \text{ GeV}$ along with the measured results.

3.5 Proton Structure Function F_2^p

We are now in a position to present the results for the proton structure function, F_2^p . In Eqs.(17,18) we presented the form of parton distributions in a CQ. Using those relations, along with the numerical values given in the Appendix, the structure function of the CQ is obtained via Eq. (1). The shape of CQ distributions in the proton is provided by Eqs.

(23) and (24). Now, all the ingredients are in place to calculate F_2^p from Eq. (20). In Figure (9) the results are shown at many values of Q^2 . As it is evident from Figure (4), sole use of CQ structure to reconstruct the F_2^p data is not enough. The CQ contribution fall a few percent short of representing the actual data. However, as mentioned earlier, there is an additional contribution from the *inherent* partons to F_2^p , which is calculated in Eq. (31). Adding this component represents the data rather well as can be seen from Figure (9). The data points are from [20]. For the purpose of comparing our results with other calculations, we have also included in Figure (9), the GRV's NLO results [21], as well as the prediction of CTEQ4M [22]. Notice that we have taken the number of active flavors to be three for $Q^2 \leq 5\text{GeV}^2$ and four, otherwise. In Figure (10), the gluon distribution predicted by the model is presented along with those from Ref.[16, 20].

4 Summary and Conclusion

In this paper we have used the notion of constituent quark as a well defined entity being common to all hadrons. Its structure can be calculated perturbatively to all orders in QCD. A CQ receives its own structure by dressing a valence quark with gluon and $q - \bar{q}$ pairs in QCD. We have calculated its structure function in the Next-to-Leading order framework. Considering a hadron as the bound states of these constituent quarks, we have used the convolution theorem to extract the hadronic structure functions for proton and pion. Besides the CQ structure contribution to the hadrons, there is also a nonperturbative contribution. This component is small, being only a few percent. But it is crucial in providing a framework to understand and explain the violation of the Gottfried sum rule and the excess of \bar{d} over \bar{u} in the nucleon sea. A mechanism is devised for this purpose and necessary calculations are performed. We have presented the results and compared them with all the available and relevant data, as well as with the work of others. We found that our results are in good agreement with the experimental data.

Acknowledgment We are grateful to professor Rudolph C. Hwa for reading the manuscript and his helpful comments and suggestions. A. N. K. is also grateful to Semnan University partially supporting his research.

5 APPENDIX

In this appendix we will give the functional form of parameters of Eqs. (17, 18) in terms of the evolution parameter, t . This will completely determines partonic structure of CQ and their evolution. The results are valid for three and four flavors, although the flavor number is not explicitly present but they have entered in through the calculation of moments. As we explained in the text, we have taken the number of flavors to be three for $Q^2 \leq 5 GeV^2$ and four for higher Q^2 values.

I) Valence quark in CQ (Eq. 17):

$$a = -0.1512 + 1.785t - 1.145t^2 + 0.2168t^3$$

$$b = 1.460 - 1.137t + 0.471t^2 - 0.089t^3$$

$$c = -1.031 + 1.037t - 0.023t^2 + 0.0075t^3$$

II) Sea quark in CQ (Eq. 18):

$$\alpha = 0.070 - 0.213t + 0.247t^2 - 0.080t^3$$

$$\beta = 0.336 - 1.703t + 1.495t^2 - 0.455t^3$$

$$\gamma = -20.526 + 57.495t - 46.892t^2 + 12.057t^3$$

$$\eta = 3.187 - 9.141t + 10.000t^2 - 3.306t^3$$

$$\xi = -7.914 + 19.177t - 18.023t^2 + 5.279t^3$$

$$\mathcal{N} = 1.023 + 0.124t - 2.306t^2 + 1.965t^3$$

III) Gluon in CQ (Eq. 18)

$$\alpha = 0.826 - 1.643t + 1.856t^2 - 0.564t^3$$

$$\beta = 0.328 - 1.363t + 0.950t^2 - 0.242t^3$$

$$\gamma = -0.482 + 1.528t - 0.223t^2 - 0.023t^3$$

$$\eta = 0.480 - 3.386t + 4.616t^2 - 1.441t^3$$

$$\xi = -2.375 + 6.873t - 7.458t^2 + 2.161t^3$$

$$\mathcal{N} = 2.247 - 6.903t + 6.879t^2 - 1.876t^3$$

References

- [1] M. Lavelle and D. McMullan, Phys. Lett. B **371**, 83 (1996) .
- [2] M. Lavelle and D. McMullan, Phys. Rep. **279**, 1 (1997).
- [3] G. Altarelli, N. Cabibbo, L. Maiani, and R. Petronzio, Nucl. Phys. B **69**, 531 (1974);
N. Cabibbo and R. Petronzio, *ibid.* **B137**, 395 (1978).
- [4] R. C. Hwa and M. S. Zahir, Phys. Rev. D **23**, 2539 (1981);
- [5] W. Furmanski, R. Petronzio, Z. Phys. **C 11**, 293 (1982).
- [6] E. G. Floratos, C. Kounnas, and R. Lacaze, Nucl. Phys. B **192** 417 (1981).
- [7] H. W. Kua, L. C. Kwek, and C. H. Oh, Phys. Rev. D **59**, 074025 (1999).
- [8] Rudolph Hwa and C. B. Yang, Phys. Rev. **C66**, 025204 (2002).
- [9] Rudolph Hwa and C. B. Yang, Phys. Rev. **C66**, 025205 (2002).

- [10] J. Magnin and H. R. Christiansen, Phys.Rev. **D61**, 054006 (2000).
- [11] H. R. Christiansen and J. Magnin, Phys. Lett. B **445** (1998) 8.
- [12] F. Arash and L. Tomio, Phys. Lett. B **401** (1997) 207 .
- [13] K. P. Das and R. C. Hwa, Phys. Lett. B **68** (1977) 459 ..
- [14] E. A. Hawker Phys. Rev. Lett. **80** (1998) 3715; J. C. Peng *et al.*, Phys. Rev. D **58** (1998) 092004.
- [15] J. S. Comway *et al.*, Phys. Rev. D **39**, 92 (1989); P. J. Sutton, A. D. Martin, W. J. Stirling, and R. G. Roberts, Phys. Rev. D **45** (1992) 2349.
- [16] NM Collab., P. Amaudruz *et al.*, Phys. Rev. Lett. **66** (1991) 2712; M. Arneodo *et al.*, Phys. Rev. D **50** (1994) R1.
- [17] G. Preparata, P. G. Ratcliffe, and J. Soffer, Phys. Rev. Lett. **66** (1991) 687.
- [18] E. M. Henley and G. A. Miller, Phys. Lett. **B 251** (1990) 453.
- [19] E. J. Eichten, I. Inchliffe and C. Quigg, Phys. Rev. D **45** (1992) 2269.
- [20] J. Breitweg, *et al.*, The Euro. Phys. Jour C **7**, 609 (1999); DESY-98-121 (1998); M. Adamus, *et al.*, ZEUS Coll., Phys.Lett. B **407**, 432 (1997); M. Derrick, *et al.*, Z. Phys. C **72**, 399 (1996); *ibid*, Z. Phys. C **65**, 293 (1995); C. Adloff, H1 Coll. *et al.*, Nucl. Phys. B **497**, 3 (1997); T. Ahmed, H1 Coll. *et al.*, Nucl. Phys. B **439**, 471 (1995), *ibid*, Nucl. Phys. B **407**, 515 (1993).
- [21] M. Gluck, E. Reya, and A. Vogt, Z. Phys. C **67**, 433 (1995).
- [22] CTEQ4, I. L. Lai, *et al.*, Phys. Rev. D **55** (1997) 1280.

6 Figure Caption

Figure-1. Moments of partons in a CQ at $Q^2 = 8.5, 25, 120 \text{ GeV}^2$. The dashed curve represents the variation of leading order moments and the solid curve is that of next to leading order.

Figure-2. Parton distributions in a CQ at a typical value of $Q^2 = 20 \text{ GeV}^2$

Figure-3. Parton distributions in proton and π^- at $Q^2 = 20 \text{ GeV}^2$ as a function of x . Here only perturbatively generated partons are presented.

Figure-4 Soft gluon distribution, xg_{soft} , as a function of x at various Q^2 values.

Figure-5. The effect of *inherent* component to a sea parton distribution in proton is presented as a function of x . The dashed-dotted line is the perturbatively generated *in-constituent quark* contribution. The solid line represents the sum of the two components.

Figure-6. Processes responsible to $SU(2)$ symmetry breaking in the nucleon sea and violation of Gottfried sum rule.

Figure-7. Pion valence structure function as a function of x at $Q^2 = 5.5 \text{ (Gev/c)}^2$. Solid curve is the result of the model calculations and the data points are from Ref.[17].

Figure-8. The ratio $\frac{\bar{d}}{\bar{u}}$ and the difference $\bar{d} - \bar{u}$ as a function of x . The solid line in the model calculation and the dotted line is the prediction of CTEQ4M [22]. Data are from Ref. [18].

Figure-9. Proton structure function F_2^p as a function of x calculated using the model and compared with the data from Ref. [20] for different Q^2 values. The dot-dot-dashed line is the prediction of GRV Ref.[21] and the dashed line is that of CTEQ4M Ref.[22].

Figure-10. The gluon distribution in proton as a function of x at $Q^2 = 20 \text{ GeV}^2$. We have also shown the prediction of GRV (dashed-dotted line) and CTEQ4M (dashed line). The data points are from H1 collaboration.

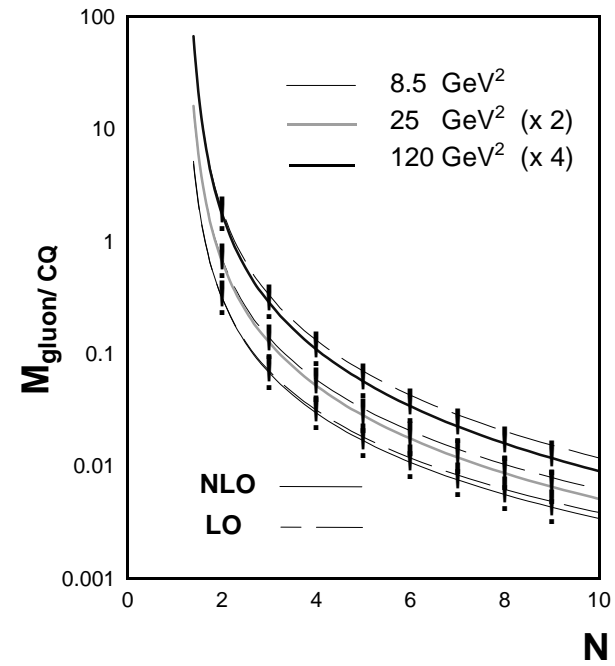
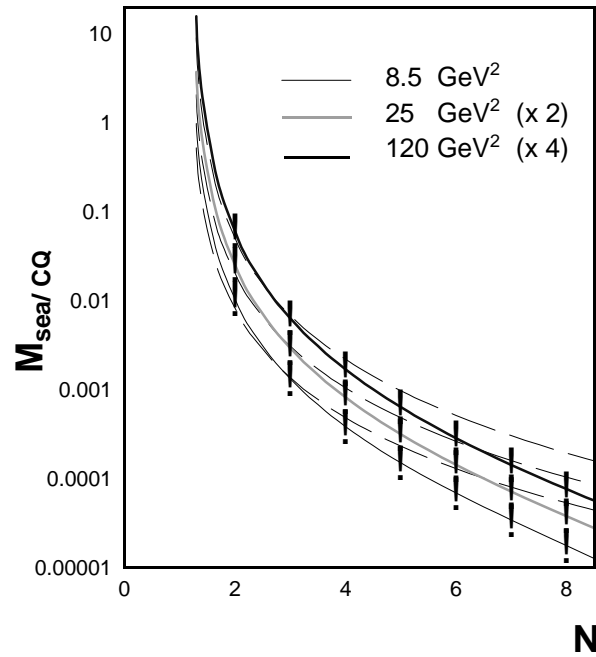
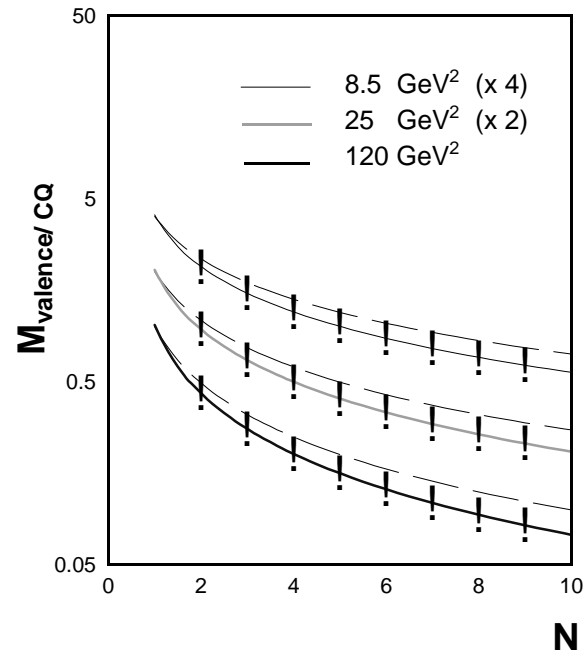


Fig. 1

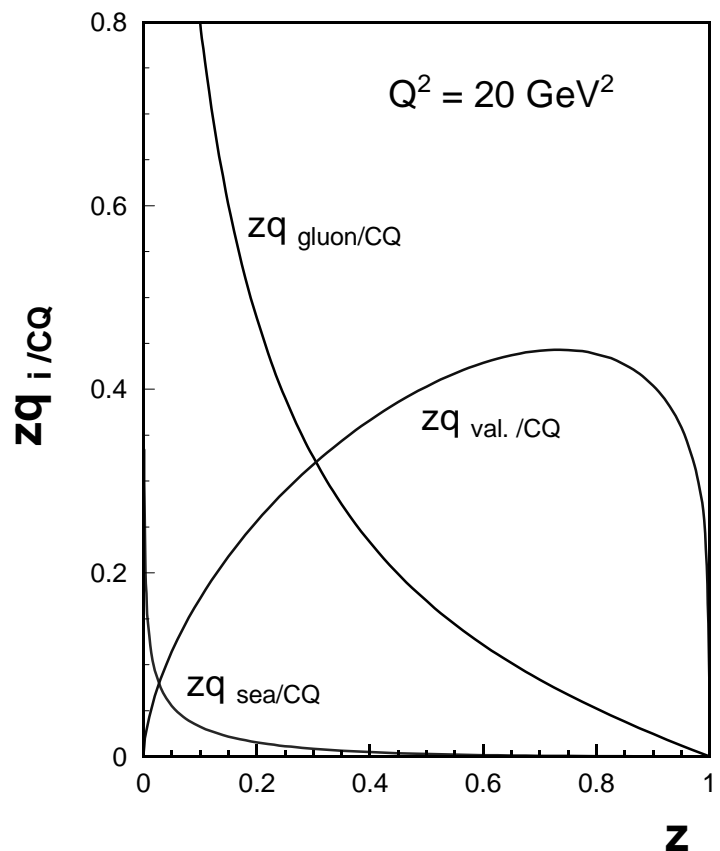


Fig. 2

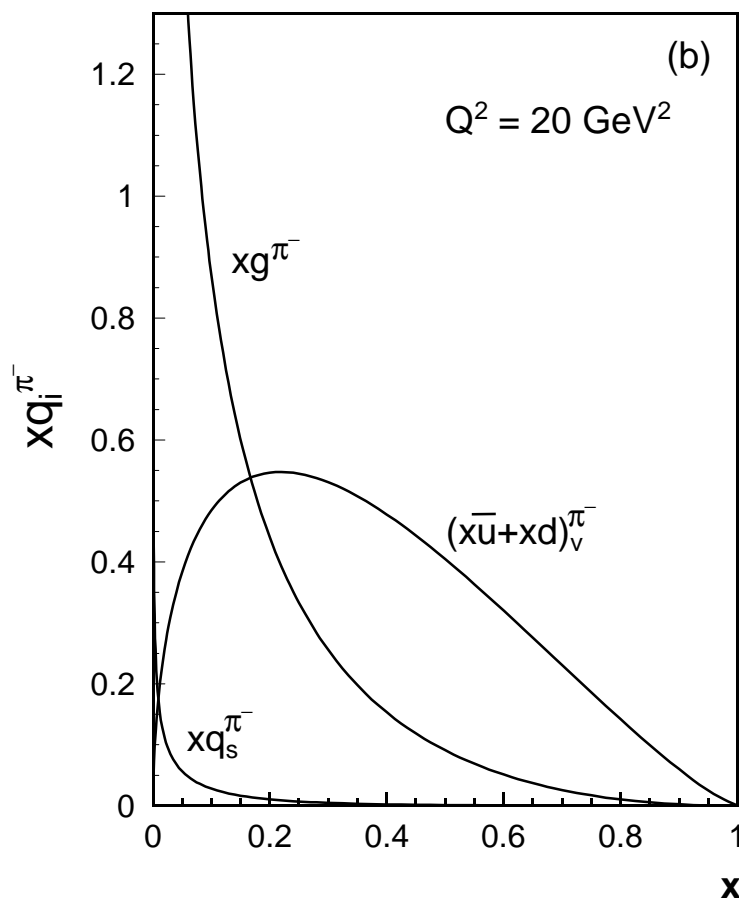
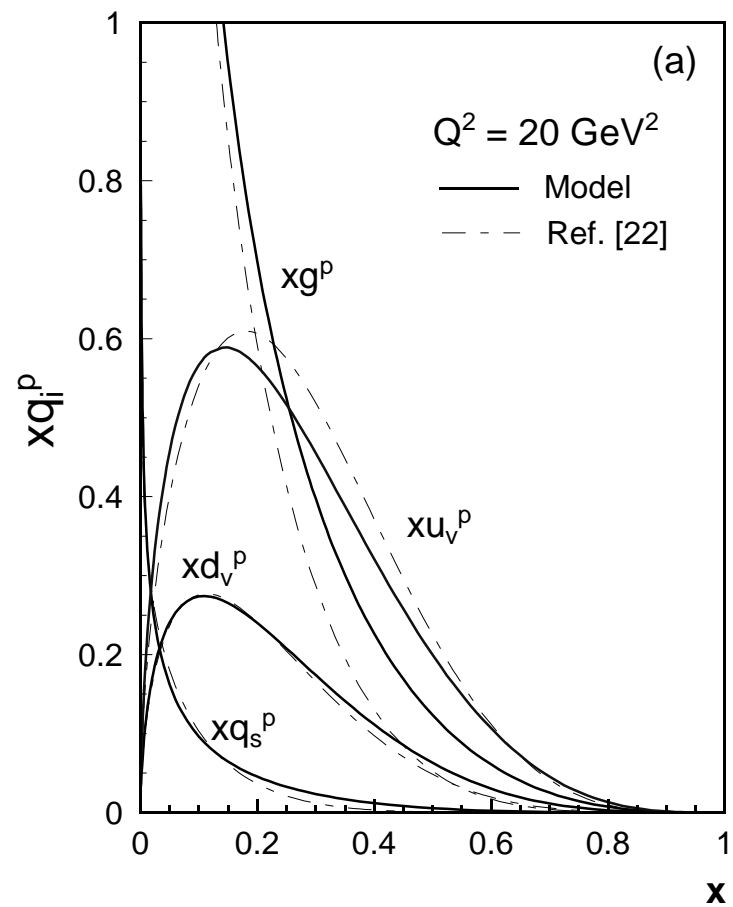


Fig. 3

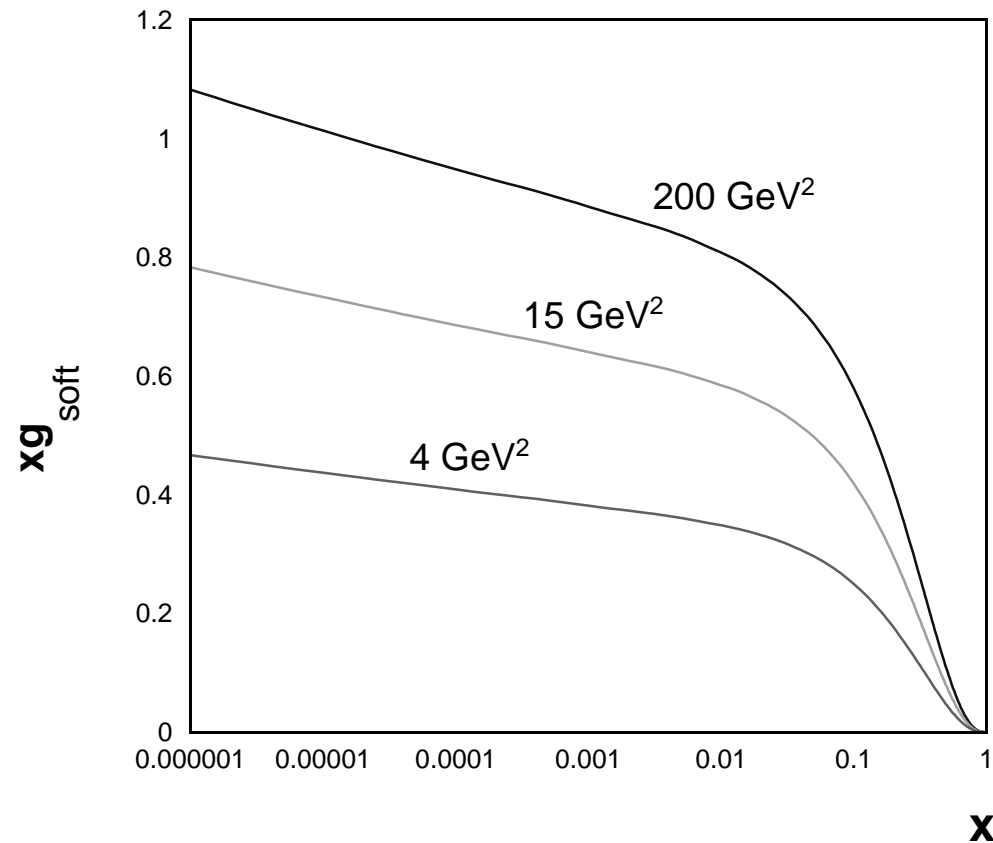


Fig. 4

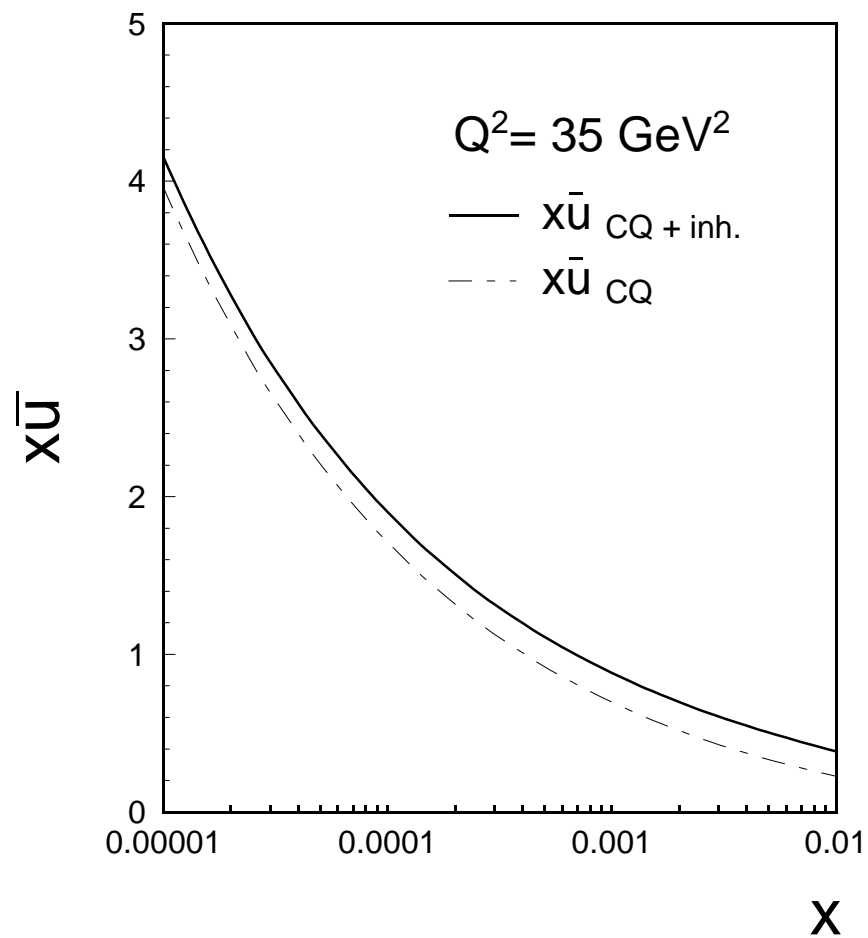


Fig. 5

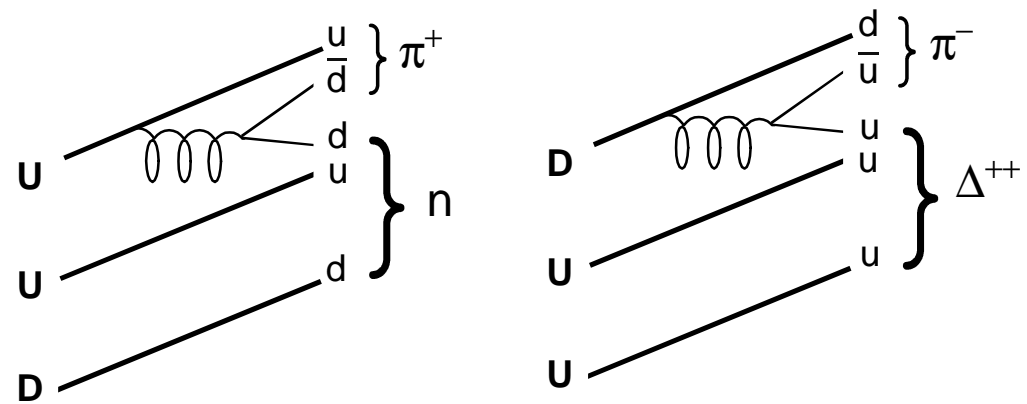


Fig. 6

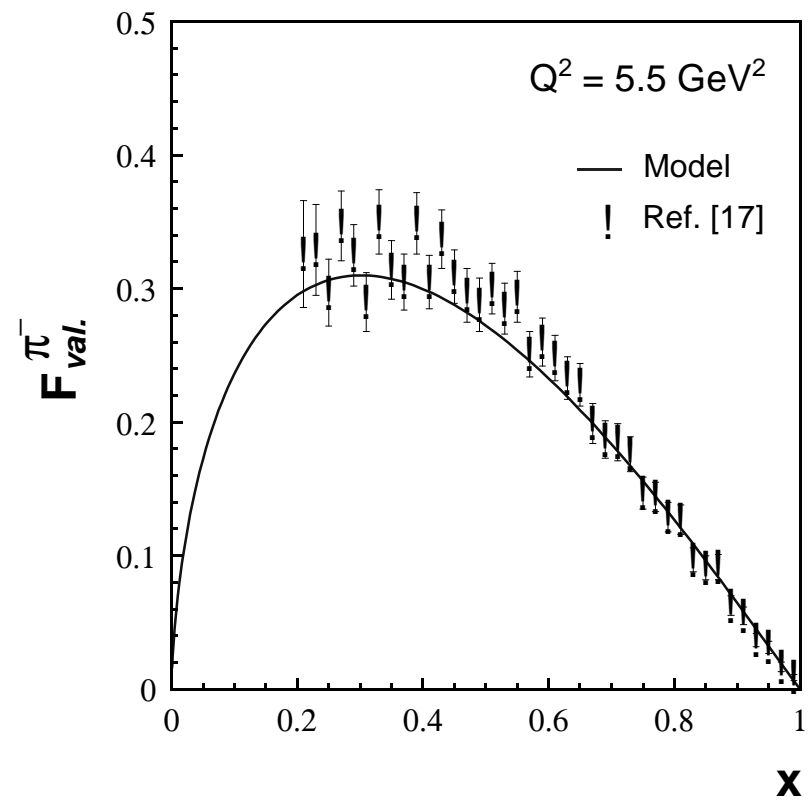


Fig. 7

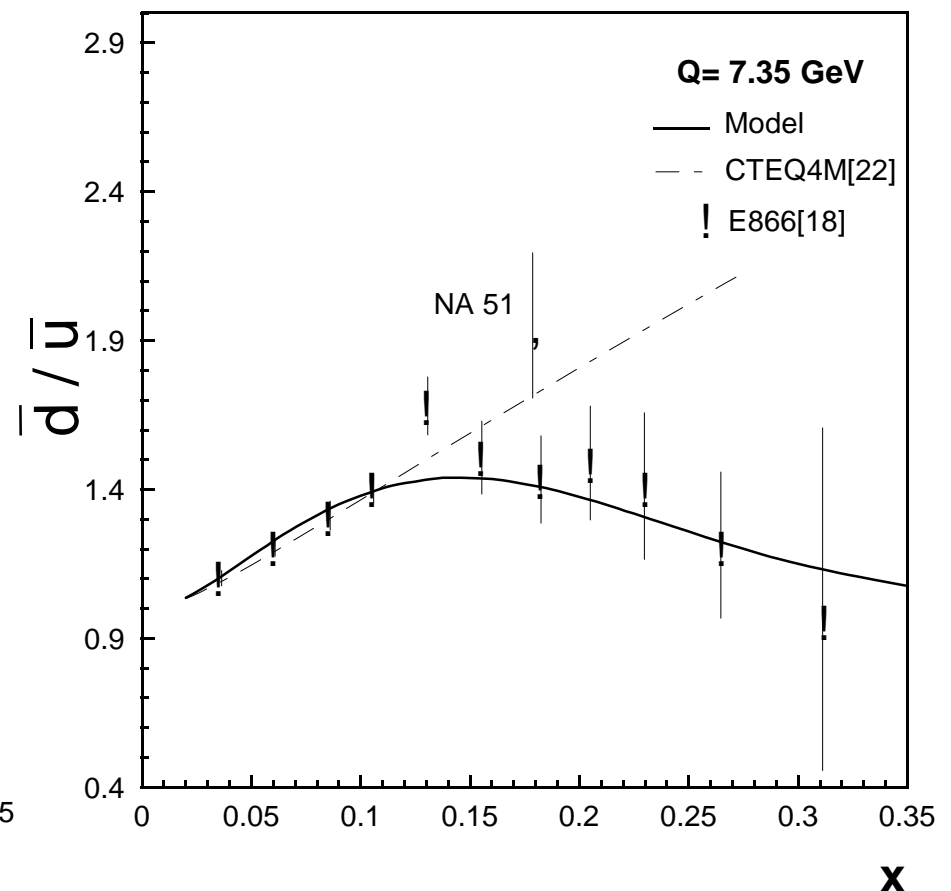
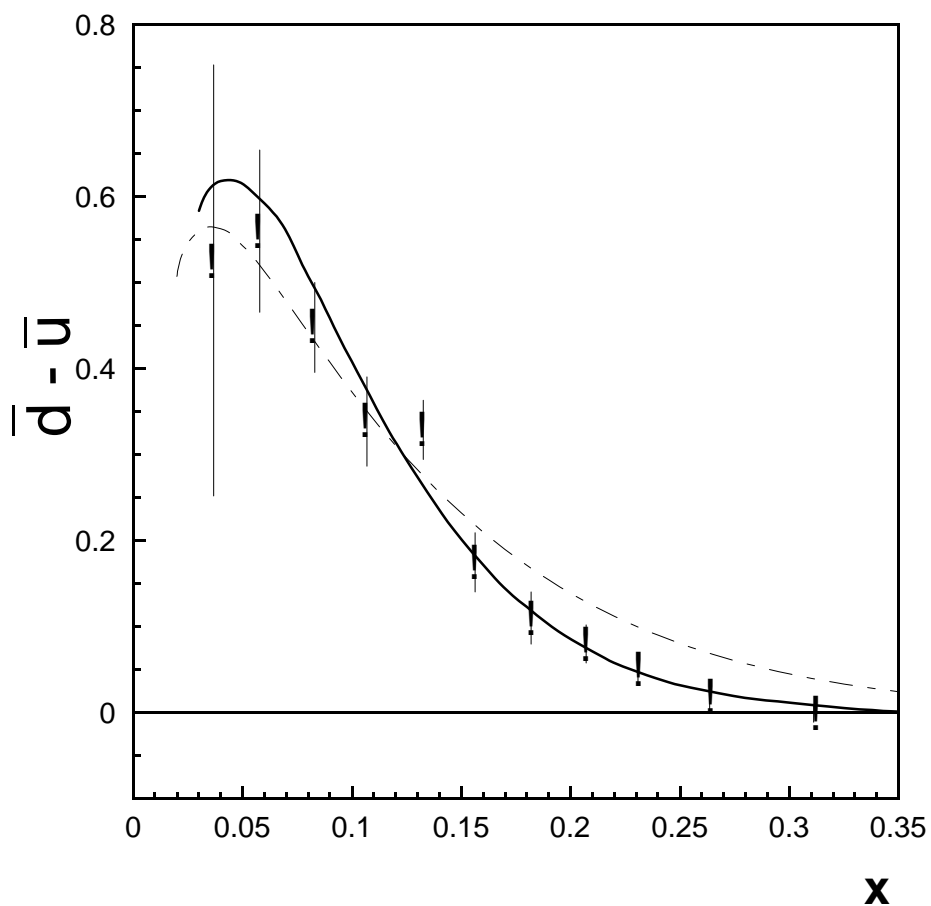


Fig. 8

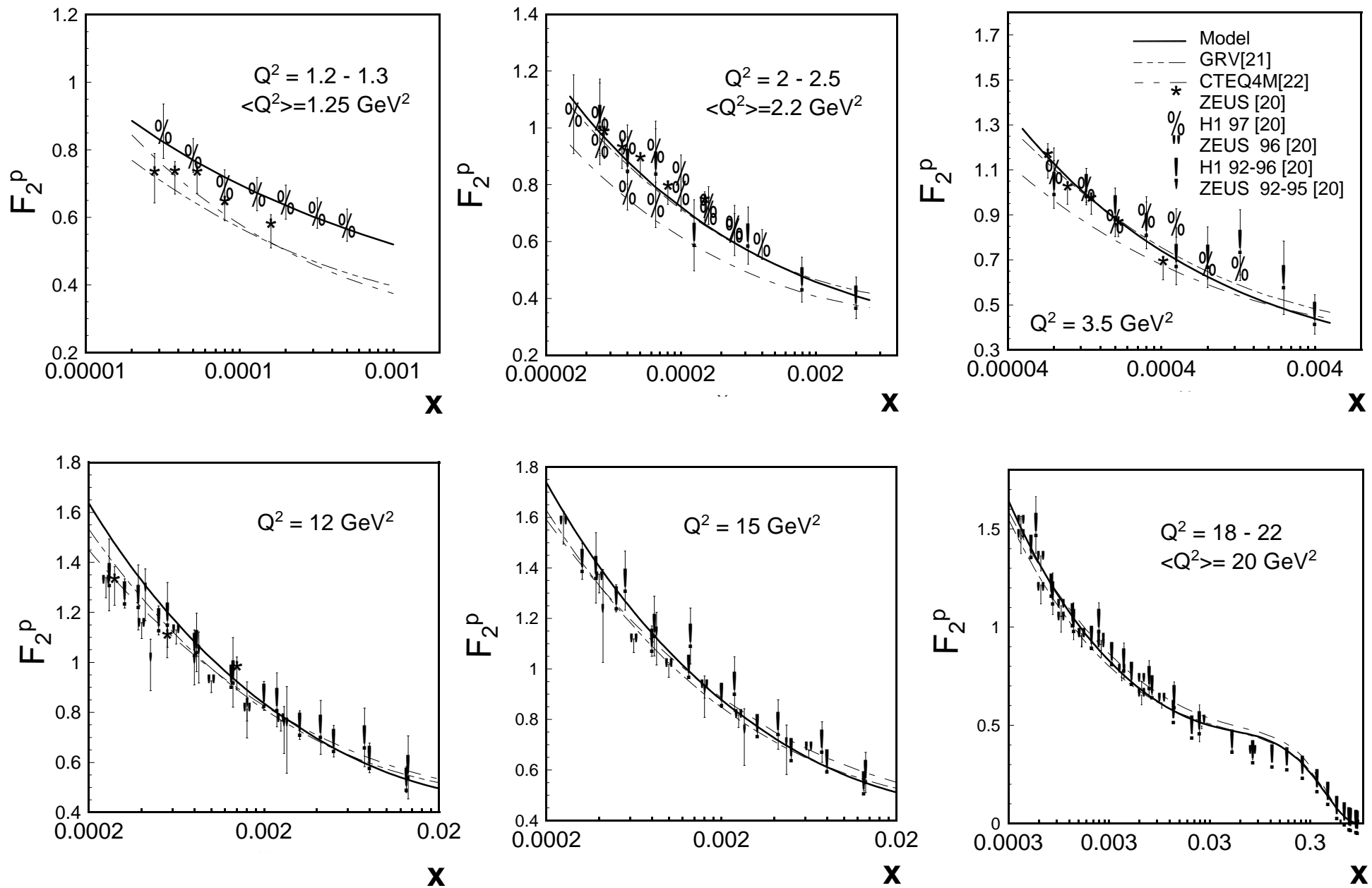


Fig. 9

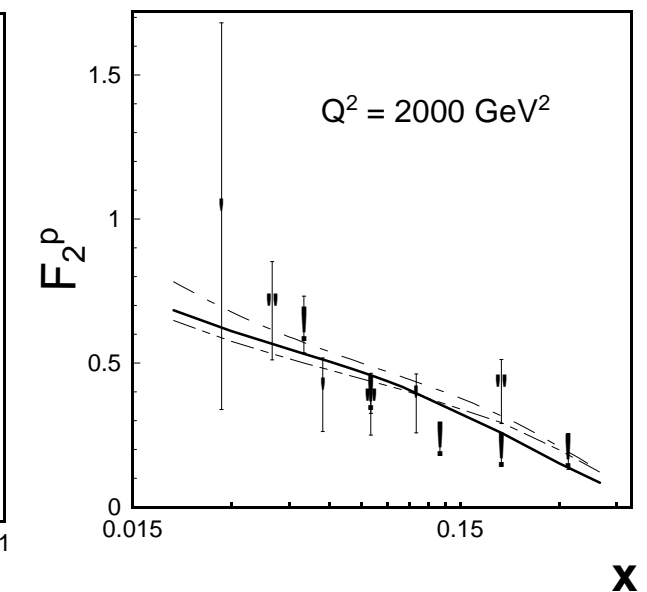
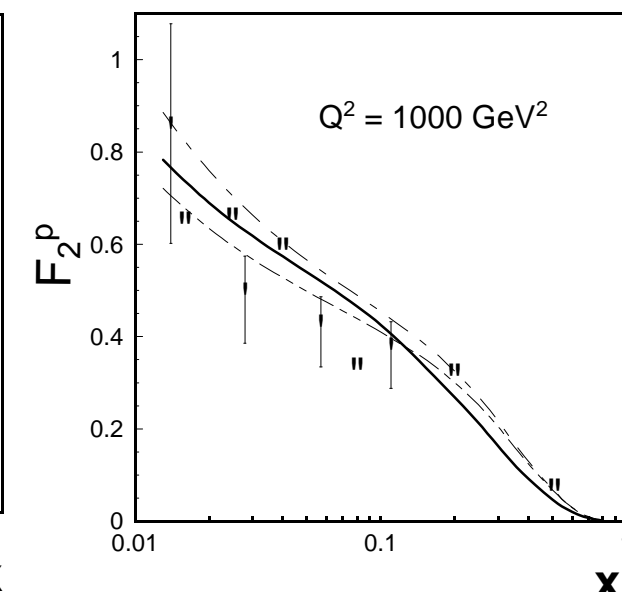
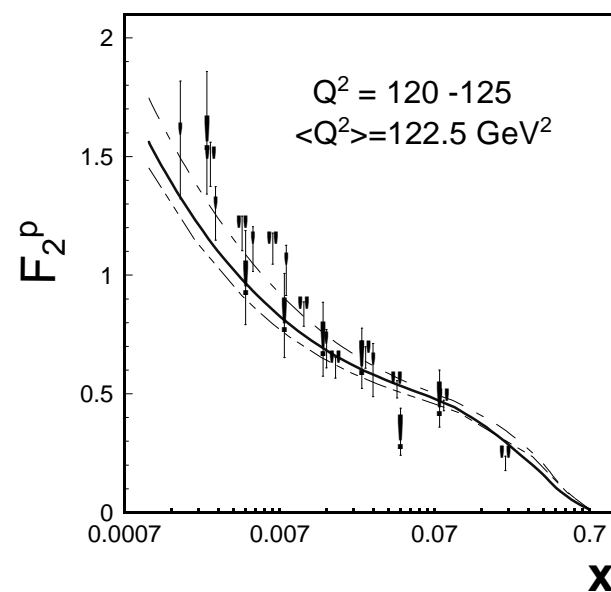
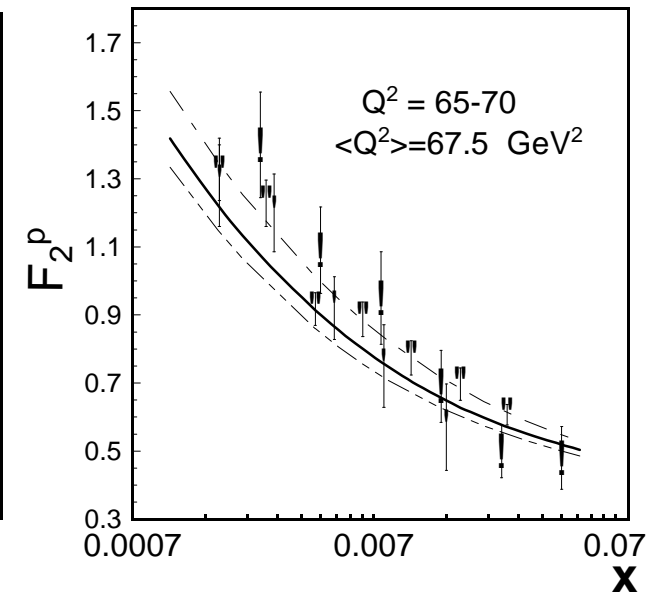
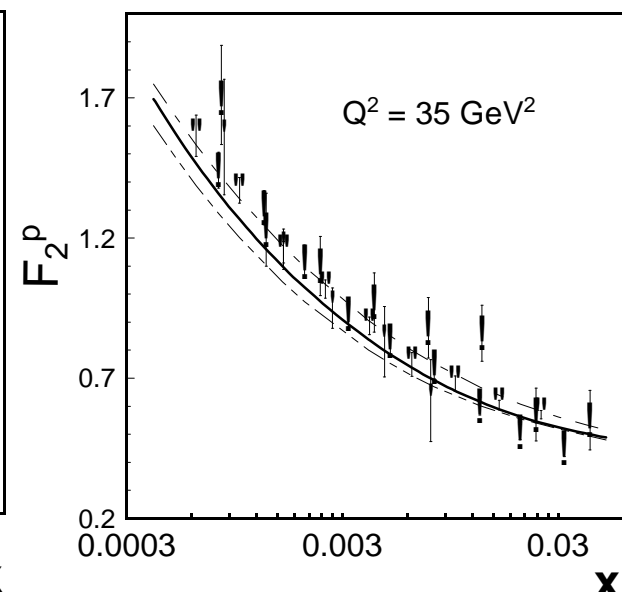
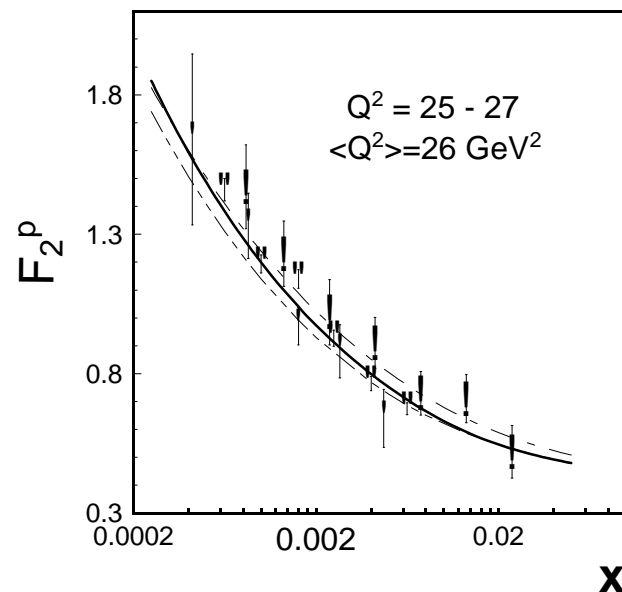


Fig. 9 (continued)

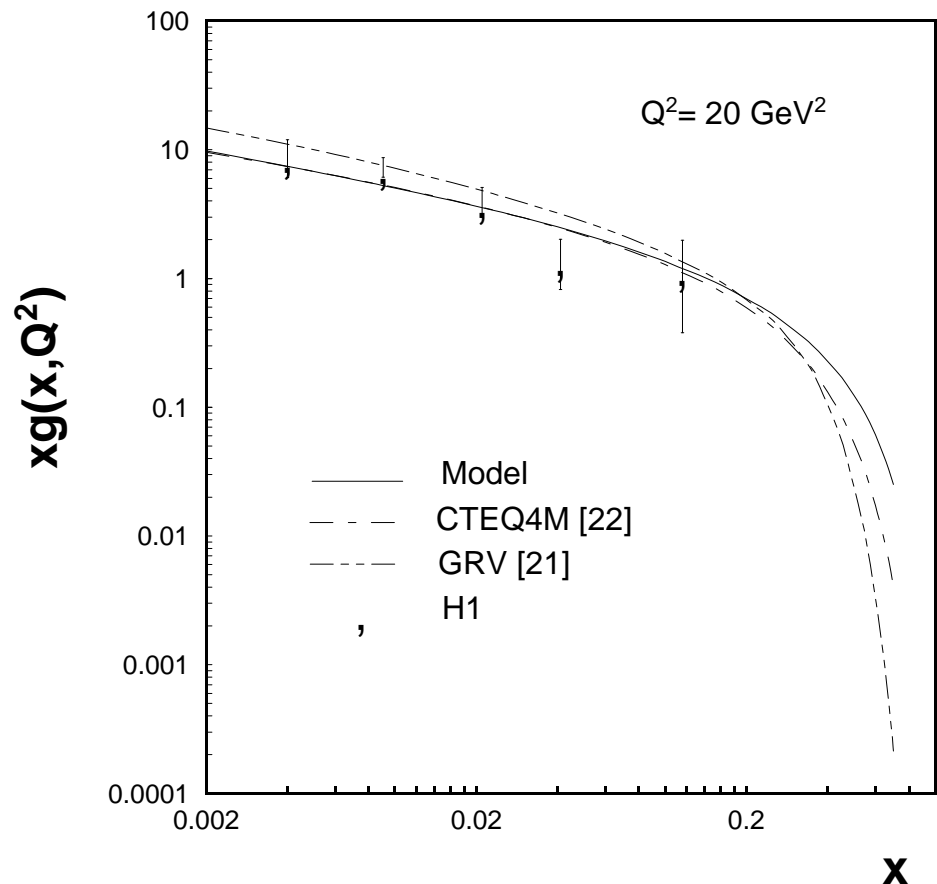


Fig.10